Tunable molecular resonances of a double quantum dot Aharonov–Bohm interferometer

2004 J. Phys.: Condens. Matter 16 117

(http://iopscience.iop.org/0953-8984/16/1/011)

INSTITUTE OF PHYSICS PUBLISHING JOURNAL OF PHYSICS: CONDENSED MATTER

J. Phys.: Condens. Matter **16** (2004) 117–124 PII: S0953-8984(04)69121-1

Tunable molecular resonances of a double quantum dot Aharonov–Bohm interferometer

Kicheon Kang[1] **and Sam Young Cho**[2]

[1] Department of Physics, Chonnam National University, Gwangju 500-757, Korea
[2] Department of Physics, University of Queensland, Brisbane 4072, Australia

Received 17 September 2003
Published 15 December 2003
Online at stacks.iop.org/JPhysCM/16/117 (DOI: 10.1088/0953-8984/16/1/011)

Abstract

We investigate resonant tunnelling through molecular states of an Aharonov–Bohm (AB) interferometer composed of two coupled quantum dots. The conductance of the system shows two resonances associated with the bonding and the antibonding quantum states. We predict that the two resonances are composed of a Breit–Wigner resonance and a Fano resonance, of which the widths and Fano factor depend on the AB phase very sensitively. Further, we point out that the bonding properties, such as the covalent and ionic bonding, can be identified by the AB oscillations.

(Some figures in this article are in colour only in the electronic version)

While single quantum dots are regarded as artificial atoms due to their quantization of energies [1, 2], two (or more) quantum dots can be coupled to form an *artificial molecule* [3]. Resonant tunnelling through serially coupled quantum dots provides some information on the coupling between dots [4], but the phase coherence of the bonding cannot be directly addressed in this geometry. Aharonov–Bohm (AB) interferometers containing a quantum dot in one of the two arms enables the investigation of the phase coherent transmission through a quantum dot [5–7]. The phase coherence of the Kondo-assisted transmission has also been studied in this geometry [8–14]. Recently, an AB interferometer set-up containing two coupled quantum dots has been realized [15]. This can be considered as the beginning point in the study of the experimentally unexplored region where various aspects of a double dot molecule can be investigated by probing the phase coherence. There are some previous theoretical works on the AB interferometer containing two quantum dots. Resonant tunnelling [16], cotunnelling [17], Kondo effect [18] and magnetic polarization current [19] have been the topics of study of the system in the absence of direct coupling between the two dots. Two-electron entanglement in the presence of direct tunnelling between the dots has also been studied [20] in relation to quantum communication.

In this paper, we study phase-sensitive molecular resonances in an Aharonov–Bohm interferometer made of two coupled quantum dots. The geometry we consider is schematically drawn in figure 1 and is equivalent to the experimental set-up of [15]. We find that the

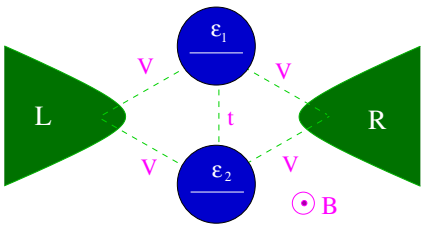

Figure 1. Schematic diagram of double quantum dots embedded in an Aharonov–Bohm interferometer.

conductance of the system consists of two molecular resonances, associated with the bonding and the antibonding quantum states. By careful analysis of the conductance as a function of energy, we argue that the two resonances are *always* composed of a Breit–Wigner resonance and a Fano resonance, with those widths and Fano factor depending very sensitively on the AB phase. Further, we point out that the bonding properties, such as the covalent and ionic bonding, can be characterized by the AB oscillations.

Our model is described by the following Hamiltonian:

$$H = H_{\mathrm{M}} + H_0 + H_{\mathrm{T}}, \tag{1a}$$

where H_{M}, H_0 and H_{T} stand for the artificial molecules of double quantum dots, two electrical leads and tunnelling between the leads and the quantum dots, respectively. For the molecule, we consider coupled non-interacting quantum dots of energies ε_1, ε_2 with a tunnelling matrix element t between them:

$$H_{\mathrm{M}} = \varepsilon_1 d_1^\dagger d_1 + \varepsilon_2 d_2^\dagger d_2 - t(d_1^\dagger d_2 + d_2^\dagger d_1), \tag{1b}$$

where d_i ($d_i^\dagger$) with $i = 1, 2$ annihilates (creates) an electron in the ith dot. The bonding properties depend on the ratio of the energy difference of the quantum dot levels ($\Delta\varepsilon \equiv \varepsilon_1 - \varepsilon_2$) and the level splitting due to tunnelling ($2t$). The molecular bonding can be called 'covalent' for $|\Delta\varepsilon| \ll 2t$, where the eigenstates of the electrons are delocalized. On the other hand, the molecule is considered to be in the 'ionic' bonding limit for $|\Delta\varepsilon| \gg 2t$, where the eigenstates are localized in one of the two dots [3]. H_0 describes the two (left and right) electrical leads modelled by the Fermi sea as

$$H_0 = \sum_{k\in\mathrm{L}} E_k^{\mathrm{L}} a_k^\dagger a_k + \sum_{k\in\mathrm{R}} E_k^{\mathrm{R}} b_k^\dagger b_k, \tag{1c}$$

where a_k ($a_k^\dagger$) and b_k ($b_k^\dagger$) annihilates (creates) an electron in the left and one in the right leads, respectively. These two leads are assumed to be identical ($E_k \equiv E_k^{\mathrm{L}} = E_k^{\mathrm{R}}$). Finally, tunnelling between the leads and the molecule is described by

$$H_{\mathrm{T}} = -\sum_{k,i=1,2} (V_{\mathrm{L}}^i d_i^\dagger a_k + \mathrm{H.c.}) - \sum_{k,i=1,2} (V_{\mathrm{R}}^i d_i^\dagger b_k + \mathrm{H.c.}). \tag{1d}$$

For simplicity, we assume that the magnitudes of the tunnelling matrix elements of the four different arms are the same (denoted by V). Then the matrix elements can be written as $V_{\mathrm{L}}^1 = V_{\mathrm{R}}^2 = V\mathrm{e}^{\mathrm{i}\varphi/4}$, $V_{\mathrm{L}}^2 = V_{\mathrm{R}}^1 = V\mathrm{e}^{-\mathrm{i}\varphi/4}$. φ represents the AB phase defined as $\varphi = 2\pi\Phi/\Phi_0$ where Φ and Φ_0 are the external flux through the interferometer and the flux quantum ($=hc/e$), respectively. The hopping strength between a quantum dot and a lead is denoted by Γ, defined as

$$\Gamma = 2\pi\rho(E_{\mathrm{F}})V^2, \tag{2}$$

where $\rho(E_{\mathrm{F}})$ stands for the density of states of each lead at the Fermi level, E_{F}.

The Hamiltonian is transformed by using the symmetric and antisymmetric modes of the leads and the quantum dots. Below it will become obvious that this approach provides better insights into the problem. Let us consider the transformations of electron operators:

$$\alpha_k = (a_k + b_k)/\sqrt{2}, \qquad \beta_k = (a_k - b_k)/\sqrt{2}, \tag{3a}$$

$$d_\alpha = (d_1 + d_2)/\sqrt{2}, \qquad d_\beta = \mathrm{i}(d_1 - d_2)/\sqrt{2}. \tag{3b}$$

Note that, for $\varepsilon_1 = \varepsilon_2$, d_α and d_β correspond to the annihilation operator of the bonding and the antibonding modes. By adopting this transformation we can rewrite the Hamiltonian as follows:

$$H = H_\alpha + H_\beta + H_{\alpha\beta}, \tag{4a}$$

where H_α, H_β take the simple form of the Fano–Anderson Hamiltonian [21] ($\gamma = \alpha, \beta$):

$$H_\gamma = \tilde{\varepsilon}_\gamma d_\gamma^\dagger d_\gamma + \sum_k E_k \gamma_k^\dagger \gamma_k + V_\gamma \sum_k (d_\gamma^\dagger \gamma_k + \gamma_k^\dagger d_\gamma). \tag{4b}$$

The energy eigenvalues of the two 'quantum dot' modes in the transformed Hamiltonian are given by $\tilde{\varepsilon}_\alpha = \varepsilon_0 - t$, $\tilde{\varepsilon}_\beta = \varepsilon_0 + t$, where $\varepsilon_0 = (\varepsilon_1 + \varepsilon_2)/2$. The hybridization matrix elements depend on the AB phase as $V_\alpha = -2V\cos(\varphi/4)$ and $V_\beta = -2V\sin(\varphi/4)$. The coupling between two modes is given by

$$H_{\alpha\beta} = -\bar{t} d_\alpha^\dagger d_\beta - \bar{t}^* d_\beta^\dagger d_\alpha, \tag{4c}$$

with the 'tunnelling' matrix element being proportional to the difference of the energy levels of the two quantum dots, $\bar{t} = \mathrm{i}(\Delta\varepsilon)/2$. It is important to note that the coupling term given in equation (4*c*) vanishes for $\varepsilon_1 = \varepsilon_2$. In other words, for the same single-particle energies of the two dots, the original Hamiltonian is mapped onto the problem of two independent Fano–Anderson Hamiltonians.

In the representation of the transformed Hamiltonian (equation (4*a*)) the dimensionless conductance can be written as [22]

$$\mathcal{G} = \tfrac{1}{4}|\Gamma_\alpha G_\alpha(E_\mathrm{F}) - \Gamma_\beta G_\beta(E_\mathrm{F})|^2 + \Gamma_\alpha\Gamma_\beta |G_{\alpha\beta}(E_\mathrm{F})|^2, \tag{5}$$

where Γ_α and Γ_β stand for the hopping strengths between the discrete level and the continuum of each mode, given by $\Gamma_\alpha = 2\Gamma\cos^2(\varphi/4)$ and $\Gamma_\beta = 2\Gamma\sin^2(\varphi/4)$, respectively. $G_\alpha(E_\mathrm{F})$ ($G_\beta(E_\mathrm{F})$) and $G_{\alpha\beta}(E_\mathrm{F})$ denote the diagonal and the off-diagonal components of the 2×2 Green function matrix. After some algebra for the Green functions we obtain a very compact form of the conductance:

$$\mathcal{G} = \frac{(e_\beta - e_\alpha)^2 + 4\Delta}{|(-e_\alpha + \mathrm{i})(-e_\beta + \mathrm{i}) - \Delta|^2}, \tag{6a}$$

where

$$e_{\alpha,\beta} \equiv \frac{2}{\Gamma_{\alpha,\beta}}(\tilde{\varepsilon}_{\alpha,\beta} - E_\mathrm{F}), \tag{6b}$$

$$\Delta \equiv \frac{4|\bar{t}|^2}{\Gamma_\alpha\Gamma_\beta} = \frac{(\Delta\varepsilon)^2}{\Gamma_\alpha\Gamma_\beta}. \tag{6c}$$

Note that equation (6*a*) reduces to the one obtained in [16] in the absence of direct coupling between two quantum dots ($t = 0$).

First we discuss the covalent bonding limit, $\varepsilon_1 = \varepsilon_2$. This limit is very instructive in providing insights into the problem, since the coupling term in the Hamiltonian (4) vanishes.

In this limit $H_{\alpha\beta} = 0$ and it is clear that the transport is associated with two resonances of widths Γ_α and Γ_β. Thus the conductance reduces to

$$\mathcal{G} = \frac{(e_\beta - e_\alpha)^2}{(e_\alpha^2 + 1)(e_\beta^2 + 1)}. \tag{7}$$

In the following we argue that for $\varepsilon_1 = \varepsilon_2$ the conductance consists of the convolution of a Breit–Wigner resonance and a Fano resonance of the two molecular (the bonding and antibonding) states. Since the hopping parameters Γ_α, Γ_β are sensitive to the AB phase, the relative strength of the resonant widths can be manipulated by the AB flux. Let us consider the limit $\Gamma_\alpha \gg \Gamma_\beta$. For the energy scale larger than Γ_β ($|e_\beta| \gg 1$), the conductance of equation (7) follows the Breit–Wigner form of its width Γ_α:

$$\mathcal{G} \simeq \mathcal{G}_{\mathrm{BW}} = \frac{1}{e_\alpha^2 + 1}. \tag{8}$$

On the other hand, one can find that the conductance shows the Fano-resonance behaviour near the antibonding state ($|e_\beta| \lesssim 1$):

$$\mathcal{G} \simeq \mathcal{G}_{\mathrm{Fano}} = \mathcal{G}_{\mathrm{b}} \frac{(e_\beta + q)^2}{e_\beta^2 + 1}, \tag{9}$$

where the Fano factor q and the background conductance $\mathcal{G}_{\mathrm{b}}$ are given by $q = 4t/\Gamma_\alpha$ and $\mathcal{G}_{\mathrm{b}} = 1/(q^2+1)$, respectively. From this analysis we find that the conductance is composed of a Breit–Wigner resonance for the bonding state ($\tilde{\varepsilon}_\alpha$) with its resonance width Γ_α and a Fano resonance for the antibonding state ($\tilde{\varepsilon}_\beta$) of width Γ_β, if $\Gamma_\alpha \gg \Gamma_\beta$. Further information is obtained from the Fano factor q. For $t = 0$ the conductance shows an antiresonance behaviour ($q = 0$), while it becomes more Breit–Wigner-like (large q) as the inter-dot coupling increases. For the other limit $\Gamma_\alpha \ll \Gamma_\beta$, the same analysis is applied with the role of the bonding and antibonding states interchanged and the Fano factor given by $q = -4t/\Gamma_\beta$. That is, for $\Gamma_\alpha \ll \Gamma_\beta$, the conductance consists of the Breit–Wigner resonance for the antibonding state and the Fano resonance near the bonding state.

Figure 2 shows the conductance as a function of the Fermi energy for three different values of t/Γ. The curve demonstrates the features described above, which follows the Breit–Wigner and Fano asymptotes for the larger and for the smaller widths of the resonances, respectively. For $\varphi = 0.3\pi$ used in figure 2, $\Gamma_\alpha \gg \Gamma_\beta$. Therefore the conductance shows Breit–Wigner behaviour for the bonding state ($E_{\mathrm{F}} \simeq \tilde{\varepsilon}_\alpha$) and Fano resonance for the antibonding state ($E_{\mathrm{F}} \simeq \tilde{\varepsilon}_\beta$). One can also verify that the Fano factor (q) increases as the bonding becomes stronger. The resonance shape for the antibonding state varies gradually from the anti-resonance for weak bonding (small q) to the Breit–Wigner-like resonance for strong bonding (large q).

Next, we investigate the more general case where $\varepsilon_1 \neq \varepsilon_2$. The same kind of analysis as for the resonances can be applied here, with the Fano resonance modified. We discuss the limit $\Gamma_\alpha \gg \Gamma_\beta$, not losing generality. For an energy scale larger than Γ_β, the conductance takes the Breit–Wigner form of equation (8), as in the $\varepsilon_1 = \varepsilon_2$ case. However, the conductance near the narrower resonance ($|e_\beta| \lesssim 1$) is modified as

$$\mathcal{G} \simeq \mathcal{G}'_{\mathrm{Fano}} = \mathcal{G}_{\mathrm{b}} \frac{|e'_\beta + Q|^2}{e'^2_\beta + 1}, \tag{10a}$$

where

$$e'_\beta = (e_\beta + \mathcal{G}_{\mathrm{b}} \Delta q)/(1 + \mathcal{G}_{\mathrm{b}} \Delta), \tag{10b}$$

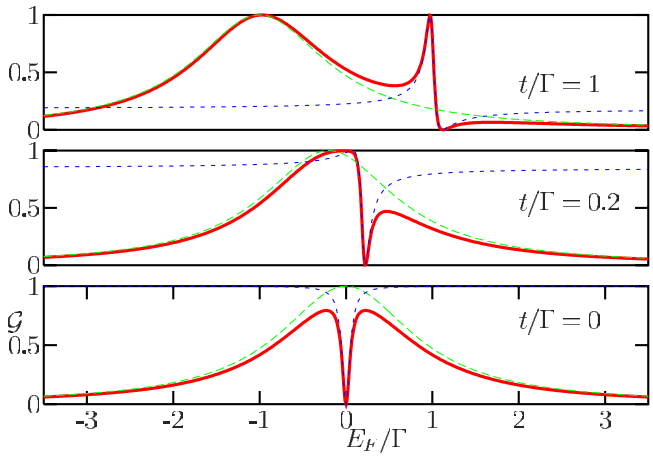

Figure 2. Dimensionless conductance ($\mathcal{G}$) as a function of the Fermi energy (full curves) for three different values of the inter-dot tunnelling ($t/\Gamma = 0, 0.2, 1$). Other parameters are given by $\varepsilon_1 = \varepsilon_2 = 0$, $\varphi = 0.3\pi$. Long and short dashed curves denote the Breit–Wigner and Fano asymptotes given in equations (8) and (9), respectively. The Fano factors for the Fano asymptotes are given by $q = 0$, 0.423 and 2.115 for $t/\Gamma = 0$, 0.2, 1, respectively.

and the modified Fano factor given by

$$Q = q\frac{1 - \mathcal{G}_b\Delta}{1 + \mathcal{G}_b\Delta} + i\frac{2\sqrt{\Delta}}{1 + \mathcal{G}_b\Delta}. \tag{10c}$$

Equation (10*a*) can be regarded as a generalized Fano resonance formula with the *complex* Fano factor Q. As pointed out in [23], the Fano factor is a complex number in the absence of time reversal symmetry, for example by applying an external magnetic field. This point was addressed experimentally with an AB interferometer containing a single quantum dot [7]. Note that the Fano factor in equation (10*c*) reduces to a real number in the absence of the magnetic field, because $\Delta \to \infty$ for $\varphi = 0$ as one can find from equation (6*c*).

Two significant changes are found in equation (10*a*) compared to equation (9).

(i) Since the modified Fano factor Q is a complex number in general, a transmission zero does not exist for $\varepsilon_1 \neq \varepsilon_2$, unlike the covalent bonding limit.
(ii) The width of the Fano resonance becomes broader due to the difference in energy levels between the dots:

$$\Gamma'_\beta = \Gamma_\beta + \mathcal{G}_b\frac{(\Delta\varepsilon)^2}{\Gamma_\alpha}. \tag{11}$$

For a fixed value of $\Delta\varepsilon$, one can find that the broadening of the resonance is significant for small inter-dot coupling, recalling the relation $\mathcal{G}_b = 1/(q^2 + 1)$ with $q = 4t/\Gamma_\alpha$.

The conductance as a function of Fermi energy for the case of different energy levels is shown in figure 3. Since $\Gamma_\alpha \gg \Gamma_\beta$ for $\varphi = 0.3\pi$, the conductance shows again the Breit–Wigner resonance behaviour for the larger energy scale corresponding to the 'bonding' state. The modified Fano resonance can be observed for the 'antibonding' state. The imaginary part of the modified Fano factor increases as the bonding strength becomes stronger, which implies that the shape of the resonance for the antibonding state varies gradually from the antiresonance to the Breit–Wigner resonance. One can also verify that the width of the Fano resonance is broader compared to the case of $\varepsilon_1 = \varepsilon_2$.

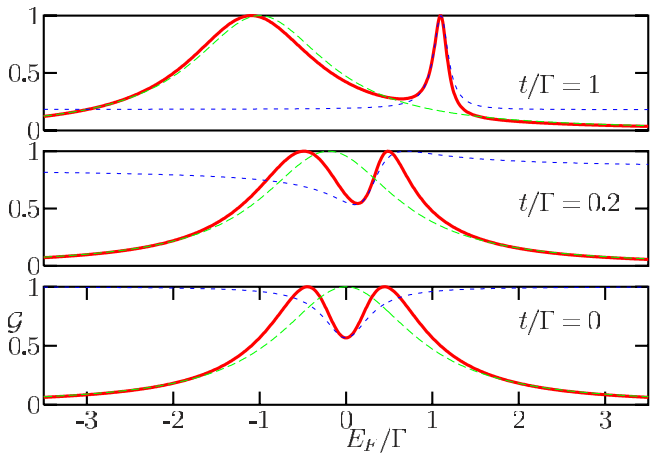

Figure 3. Dimensionless conductance ($\mathcal{G}$) as a function of the Fermi energy (full curves) for three different values of the inter-dot tunnelling ($t/\Gamma = 0, 0.2, 1$). Other parameters are given by $\varepsilon_1 = -0.5\Gamma$, $\varepsilon_2 = 0.5\Gamma$, $\varphi = 0.3\pi$. Long and short dashed curves denote the Breit–Wigner and generalized Fano asymptote given by equations (8) and (10*a*), respectively. The generalized Fano factors for the asymptotes are given by $Q = 0.753\text{i}$, $-0.258 + 0.861\text{i}$, $0.128 + 2.335\text{i}$ for $t/\Gamma = 0, 0.2, 1$, respectively.

Finally, we discuss the Aharonov–Bohm oscillations of the conductance for the molecular states and show that information about the bonding properties can be obtained by the oscillation patterns. As shown in figure 4, the oscillation patterns of the ionic bonding limit are very different from those of the covalent bonding limit. Above all, the periodicity is 2π in the ionic bonding limit while it becomes 4π in the covalent bonding limit. This periodicity variation can be interpreted in terms of the effective coupling strength between the two dots. In the ionic bonding limit of $|\Delta\varepsilon| \gg 2t$, the AB oscillation has the usual 2π periodicity since the coupling between the dots is ineffective. However, in the covalent bonding limit, the coupling between dots becomes important and this strong effective coupling separates the interferometer into two sub-regions with their cross-sectional area halved. Therefore the oscillation period is doubled.

Comparing the AB oscillations of the bonding (figure 4(b)) and the antibonding (figure 4(c)) states, one finds that there are phase differences of 2π between the corresponding eigenstates. This originates from the difference of the wavefunction symmetry of the two eigenstates.

It should be noted that our discussions on the AB oscillation characterizing the bonding properties (ionic, covalent) can be applied only when the two regions divided by the direct tunnelling have the same area. Though it seems possible to have devices with the same effective areas from the current nanofabrication technology, the two regions may have different areas in practice. In this case, the AB oscillations become more complicated and will show a kind of 'quantum beating' originating from the difference in area, which we do not address further here.

In conclusion, we have investigated resonant tunnelling through the molecular states in an Aharonov–Bohm interferometer composed of two coupled quantum dots. We have found that the two resonances are composed of a Breit–Wigner resonance and a Fano resonance, for which the widths and the Fano factor depend on the AB phase. Further, we have suggested that the bonding properties and their symmetries can be characterized by the AB oscillation.

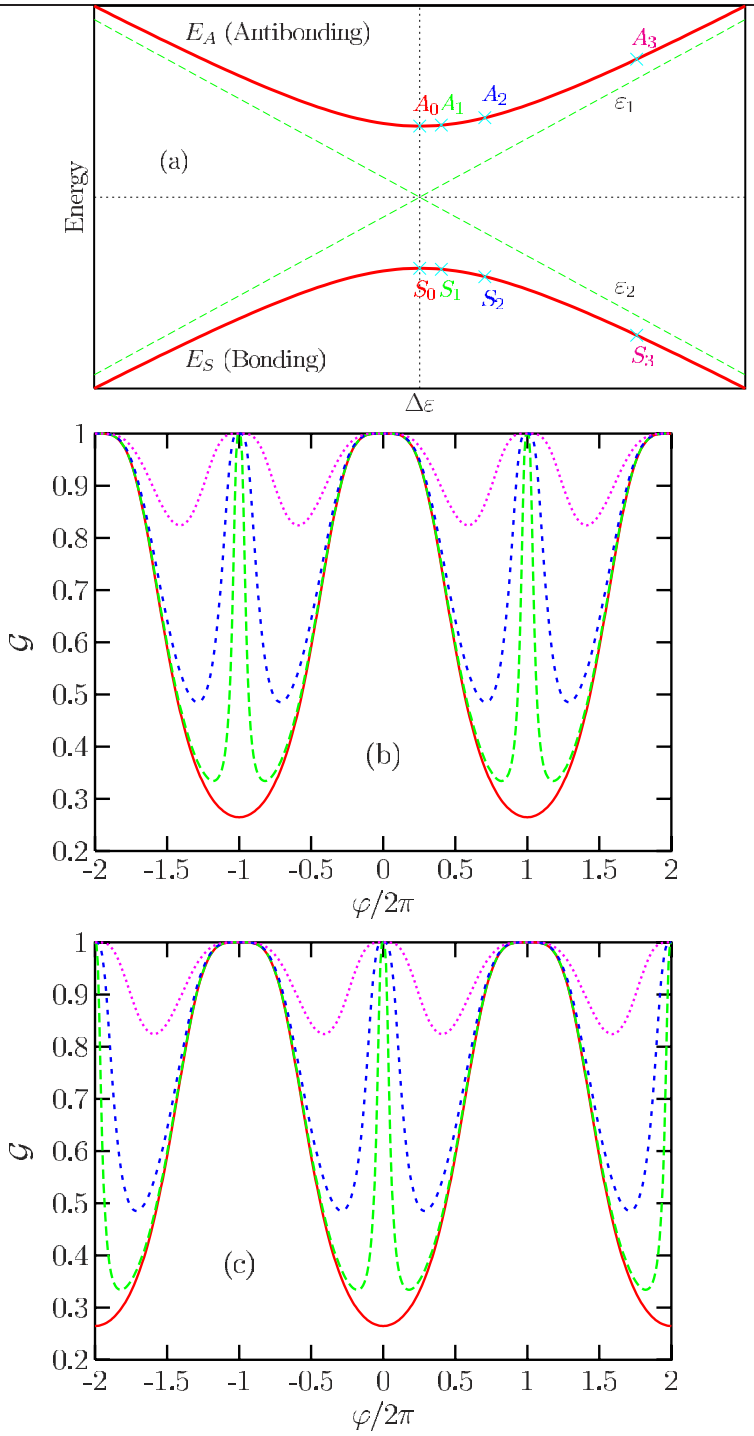

Figure 4. (a) Molecular two-level energies as a function of the difference between the energy levels of the quantum dots. (b) AB oscillations for the bonding states with $\Delta\varepsilon/t = 0$ (full curve), $\Delta\varepsilon/t = 1/3$ (long dashed curve), $\Delta\varepsilon/t = 1$ (short dashed curve) and $\Delta\varepsilon/t = 10/3$ (dotted curve), marked in (a) as S_0, S_1, S_2 and S_3, respectively. (c) AB oscillations for the antibonding states with $\Delta\varepsilon/t = 0$ (full curve), $\Delta\varepsilon/t = 1/3$ (long dashed curve), $\Delta\varepsilon/t = 1$ (short dashed curve) and $\Delta\varepsilon/t = 10/3$ (dotted curve), marked in (a) as A_0, A_1, A_2 and A_3, respectively.

Acknowledgments

We wish to acknowledge H-W Lee for useful discussions and comments. This work has been supported by the Korean Ministry of Information and Communication.

References

[1] Kastner M A 1993 *Phys. Today* **46** (1) 24
[2] Kouwenhoven L P, Austing D G and Tarucha S 2001 *Rep. Prog. Phys.* **64** 701
[3] For a review see e.g. van der Wiel W G, De Franceschi S, Elzerman J M, Fujisawa T, Tarucha S and Kouwenhoven L P 2003 *Rev. Mod. Phys.* **75** 1
[4] van der Vaart N C *et al* 1995 *Phys. Rev. Lett.* **74** 4702
[5] Yacoby A, Heiblum M, Mahalu D and Shtrikman H 1995 *Phys. Rev. Lett.* **74** 4047
[6] Schuster R, Buks E, Heiblum M, Mahadu D, Umansky V and Shtrikman H 1997 *Nature* **385** 417
[7] Kobayashi K, Aikawa H, Katsumoto S and Iye Y 2002 *Phys. Rev. Lett.* **88** 256806
[8] van der Wiel W G, De Franceschi S, Fujisawa T, Elzerman J M, Tarucha S and Kouwenhoven L P 2000 *Science* **289** 2105
[9] Ji Y, Heiblum M, Sprinzak D, Mahalu D and Shtrikman H 2000 *Science* **290** 779
Ji Y, Heiblum M and Shtrikman H 2002 *Phys. Rev. Lett.* **88** 076601
[10] Gerland U, von Delft J, Costi T A and Oreg Y 2000 *Phys. Rev. Lett.* **84** 3710
[11] Kang K and Shin S-C 2000 *Phys. Rev. Lett.* **85** 5619
Cho S Y, Kang K, Kim C K and Ryu C-M 2001 *Phys. Rev.* B **64** 033314
Kang K, Cho S Y and Park K W 2002 *Phys. Rev.* B **66** 075312
[12] Bulka B R and Stefański P 2001 *Phys. Rev. Lett.* **86** 5128
[13] Hofstetter W, König J and Schoeller H 2001 *Phys. Rev. Lett.* **87** 156803
[14] Kang K and Craco L 2002 *Phys. Rev.* B **65** 033302
[15] Holleitner A W, Decker C R, Qin H, Eberl K and Blick R H 2001 *Phys. Rev. Lett.* **87** 256802
Holleitner A W, Blick R H, Hüttel A K, Eberl K and Kotthaus J P 2002 *Science* **297** 70
[16] Kubala B and König J 2002 *Phys. Rev.* B **65** 245301
[17] Akera H 1993 *Phys. Rev.* B **47** 6835
[18] Izumida W, Sakai O and Shimizu Y 1997 *J. Phys. Soc. Japan* **66** 717
[19] Cho S Y, McKenzie R H, Kang K and Kim C K 2003 *J. Phys.: Condens. Matter* **15** 1147
[20] Loss D and Sukhorukov E V 2000 *Phys. Rev. Lett.* **84** 1035
[21] See, for example, Mahan G D 1990 *Many-Particle Physics* 2nd edn (New York: Plenum)
[22] Meir Y and Wingreen N S 1992 *Phys. Rev. Lett.* **68** 2512
[23] Clerk A A, Waintal X and Brouwer P W 2001 *Phys. Rev. Lett.* **86** 4636